

## Invisible lenses with positive isotropic refractive index

Tomáš Tyc,<sup>1,\*</sup> Huanyang Chen,<sup>2</sup> Aaron Danner,<sup>3</sup> and Yadong Xu<sup>2</sup>

<sup>1</sup>*Faculty of Science and Faculty of Informatics, Masaryk University, Kotlářská 2, 61137 Brno, Czech Republic*

<sup>2</sup>*College of Physics, Optoelectronics and Energy, Soochow University, Suzhou, 215006 Jiangsu, China*

<sup>3</sup>*Department of Electrical and Computer Engineering, National University of Singapore, Singapore 117583*

(Received 8 September 2014; revised manuscript received 30 September 2014; published 14 November 2014)

We analyze the optical properties of the so-called invisible lenses in the wave-optics regime and show that they are practically invisible for a discrete set of frequencies. For other frequencies, the phase delay of the waves that pass through the lens compared to those that do not disturbs the outgoing waves. The frequencies for which the lens is invisible are influenced by the Gouy phase. This is the only known invisible device made of positive isotropic material at finite frequencies.

DOI: [10.1103/PhysRevA.90.053829](https://doi.org/10.1103/PhysRevA.90.053829)

PACS number(s): 42.25.Fx, 42.15.Eq

### I. INTRODUCTION

Invisibility is the ultimate optical illusion, where light rays propagate around an object through an optical medium that surrounds it—the invisible cloak—and then resume their original directions and transversal positions. In this way, the rays beyond the object surrounded by the invisible cloak move in the same way as if the object and the cloak were not present at all, and an observer therefore sees “through” the object. Since the discovery of invisible cloaking in 2006 [1,2], a large number of cloaks of different types have been proposed, including non-Euclidean cloaks [3], carpet cloaks [4,5], subluminal cloaks [6], and cloaks based on negative permittivity [7] and negative refractive index [8] materials. The cloaks that work for all directions of the incoming rays are composed of materials that are either highly anisotropic or with negative material parameters; almost isotropic materials can be employed only in the case of carpet cloaks that work just for a limited range of directions.

Despite that, there exists a class of objects that consist of an isotropic optical material and still are invisible, at least within geometrical optics. These objects have a spherically symmetric refractive index profile and the simplest one of them is described in the literature as the invisible lens [9,10]. Figure 1(a) shows rays propagating in this lens. Although the invisible lens cannot function as an invisible cloak because there is no room in it to include another object to become invisible, the fact that a device formed of an isotropic material may be invisible is remarkable.

So far, the invisibility properties of the invisible lens have been derived from the behavior of light rays propagating in it. This is reasonable in the geometrical optics limit of  $\lambda \ll a$ , where  $\lambda$  is the wavelength of light and  $a$  is the radius of the lens, but not if  $\lambda$  and  $a$  become comparable. The purpose of this paper is to investigate the properties of the invisible lens in the long-wavelength regime and show that for certain discrete frequencies, it is practically invisible even in the full wave description. This demonstrates the fact that optically isotropic invisible objects are possible.

### II. THE INVISIBLE LENS

We begin our analysis with the two-dimensional (2D) version of the invisible lens. It has the refractive index [10]

$$n(r) = \left( Q - \frac{1}{3Q} \right)^2, \quad Q = \sqrt[3]{-\frac{a}{r} + \sqrt{\frac{a^2}{r^2} + \frac{1}{27}}}, \quad (1)$$

where  $r$  is the radial coordinate. The index value at the boundary,  $n(a) = 1$ , matches the index of the environment, so there is no refraction or reflection at the lens boundary and the rays smoothly enter the lens. The refractive index diverges as  $n(r) \approx (2/r)^{2/3}$  at  $r = 0$ , but this singularity can be eliminated by the method of transmutation of singularities [11] at the expense of introducing a slight anisotropy of the index. In the regime of geometrical optics, a light ray that hits the lens makes a loop around its center and exits at exactly the same direction as it entered, without any transverse shift; see Fig. 1(a). This way the ray, after leaving the lens, propagates as if it had propagated just through an empty space, which makes the device invisible within geometrical optics. The only disturbance is a time (or, equivalently, phase) delay of the rays that entered the lens compared to those that did not. This delay is constant because rays are perpendicular to the wave fronts, and equal to  $\Delta t = 2\pi a/c$ , as can be verified easily for the outermost ray hitting the lens with impact parameter  $a$ .

### III. WAVES IN THE INVISIBLE LENS

Since there is a time delay of the rays that entered the invisible lens, we can expect a phase slip at the border of the lens “shadow” if it is illuminated by light waves. (By “shadow” we mean the region occupied by the rays from the source that passed through the lens.) If the time delay equals an integer multiple of the wave period  $2\pi/\omega$ , then we can expect at the boundary of the shadow a constructive interference of the waves that passed through the lens and those that did not. Otherwise, the interference will be at least partially destructive and the wave will be disturbed. This gives a condition for which we can expect the lens to be invisible in the wave-optics regime,

$$\omega = Nc/a, \quad N \in \mathbb{N}. \quad (2)$$

\*tomtyc@physics.muni.cz

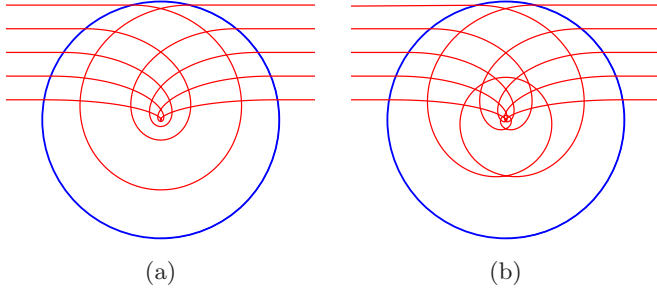


FIG. 1. (Color online) Rays in the (a) invisible lens and (b) double invisible lens.

To see whether this simple argument is valid, consider a monochromatic plane wave  $\psi_{\text{in}} = \exp[i(kx - \omega t)]$  incident on the lens that is centered at the origin of coordinates. For simplicity, we consider scalar waves. The total wave  $\psi_{\text{tot}}$  outside the lens (in the region  $r \geq 1$ ) can be written as a sum of the incoming wave  $\psi_{\text{in}}$  and a scattered wave  $\psi_{\text{scatt}}$ . To find the scattered wave, we use the partial-wave expansion and expand the plane wave  $\psi_{\text{in}}$  as a superposition of cylindrical waves [we omit the time factor  $\exp(-i\omega t)$  in the following]:

$$\psi_{\text{in}} = \exp(ikx) = \sum_{m=-\infty}^{\infty} i^m J_m(kr) \exp(im\varphi), \quad (3)$$

where  $J_m$  are the Bessel functions. Each term in this sum can be expressed as a sum of a converging and diverging cylindrical wave described by Hankel functions due to the identity

$$J_m(kr) = \frac{1}{2} [H_m^{(2)}(kr) + H_m^{(1)}(kr)]. \quad (4)$$

If we imagine for a moment that the invisible sphere is not present yet (so the refractive index  $n = 1$  in the whole 2D space), we can think of the expansion (3) with Eq. (4) substituted into it, as if for each  $m$  there is a converging cylindrical wave  $i^m H_m^{(2)}(kr) \exp(im\varphi)/2$  that changes into a diverging wave  $i^m H_m^{(1)}(kr) \exp(im\varphi)/2$  at the origin. Now when we put the invisible sphere at the origin, the converging cylindrical wave will still be the same, but the diverging wave will now be phase shifted compared to the situation without the lens present. If we denote this shift by  $\alpha_m$ , we get the total wave

$$\psi_{\text{tot}} = \sum_{m=-\infty}^{\infty} \frac{i^m}{2} [H_m^{(2)}(kr) + H_m^{(1)}(kr) \exp(i\alpha_m)] \exp(im\varphi). \quad (5)$$

The scattered wave is then the difference between Eqs. (5) and (3),

$$\psi_{\text{scatt}} = \sum_{m=-\infty}^{\infty} i^m \frac{\exp(i\alpha_m) - 1}{2} H_m^{(1)}(kr) \exp(im\varphi). \quad (6)$$

The strength with which the invisible sphere scatters the  $m$ th cylindrical component can be quantified by the square of the magnitude of the coefficient in front of  $H_m^{(1)}(kr)$ , i.e., of the fraction in Eq. (6). This evaluates to  $S_m = \cos^2(\alpha_m/2)$ . To give little scattering at some frequency  $\omega$ , the quantities  $S_m$  should be small.

To see how the invisible sphere behaves in waves incident on it, we have numerically calculated the quantities  $S_m$

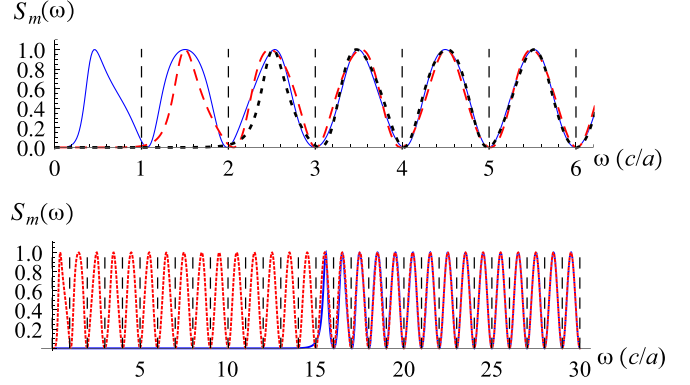


FIG. 2. (Color online) The coefficients  $S_m(\omega)$  for different values of  $m$  with  $\omega$  shown in the units  $c/a$ . The top picture shows the cases for  $m = 0, 1$ , and  $2$  (full blue line, dashed red line, and dotted black line, respectively). The bottom picture shows the cases for  $m = 0$  and  $15$  (dotted red line and full blue line, respectively) on a larger interval of frequencies. The vertical dashed lines mark the positions of integer frequencies satisfying condition (2).

as functions of frequency  $\omega$  for different values of  $m$ . For this purpose, we found the numerical solutions of the Helmholtz equation  $[\Delta + \omega^2 n(r)^2/c^2]\psi = 0$  in the medium with refractive index (1) in the region  $r \leq 1$ . This solution (with a free multiplication factor) was then matched to a superposition of the Hankel functions  $H_m^{(1)}(kr)$  and  $H_m^{(2)}(kr)$  [the  $m$ th term in Eq. (5)] to get a function that is continuous at  $r = 1$  including its derivative. In this way, we obtained the coefficients  $S_m$  as well as the semianalytical solution of the Helmholtz equation for each  $m$ , and were then able to construct the total wave as a superposition of these solutions.

Figure 2 shows the calculated coefficients  $S_m(\omega)$  for several values of  $m$  (we are using the units in which  $c = a = 1$ ). Remarkably,  $S_m(\omega)$  are all very small for integer  $\omega$ , which are exactly the frequencies satisfying the condition (2). This means that at the integer frequencies, we can indeed expect negligible scattering from the invisible lens. This is demonstrated in Figs. 3(a) and 3(b) that show the plot of the wave calculated by our method for two integer values of  $\omega$ . At the same time, at half-integer frequencies, the coefficients  $S_m(\omega)$  are large, which suggests a stronger scattering. The plot of the waves in this case for two half-integer values of  $\omega$  can be seen in Figs. 3(c) and 3(d). The phase slip at the boundary of the shadow is clearly visible. This makes the performance of the invisible lens similar to that of a non-Euclidean cloak [12] and a conformal cloak [13]. There, similarly as here, the invisibility is very good for a discrete set of frequencies where the rays that have entered the cloak interfere constructively with those that have not.

Figure 4 shows the waves for larger frequencies, namely, for  $\omega = 20$  and  $\omega = 20.5$ . We see again that for integer frequency, the invisibility is almost perfect, while for half-integer frequency, the wave is disturbed at the boundary of the lens shadow. The fact that the lens is not completely invisible even at the integer frequencies is unavoidable due to the theorem of the uniqueness of the inverse-scattering problem for waves [14].

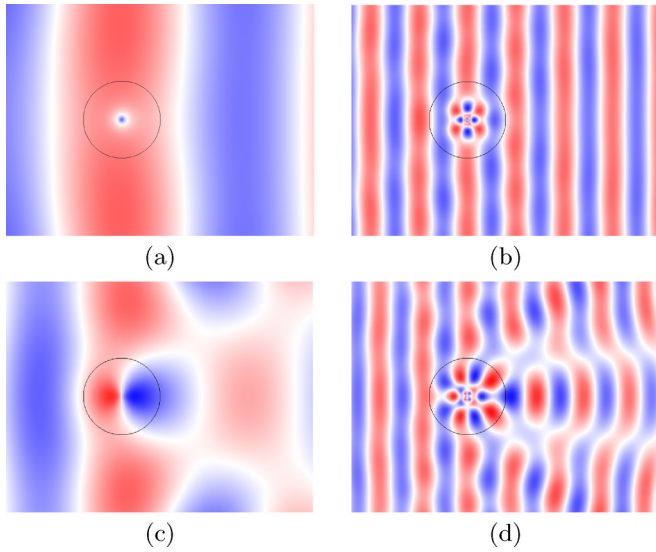


FIG. 3. (Color online) Plot of the waves resulting from illumination of the 2D invisible lens by a plane wave from the left for (a)  $\omega = 1$ , (b)  $\omega = 5$ , (c)  $\omega = 1.5$ , and (d)  $\omega = 5.5$ . In the cases (a) and (b), the lens is practically invisible; in (c) and (d), there is a phase slip along the shadow boundary. The border of the lens is marked by the black circle.

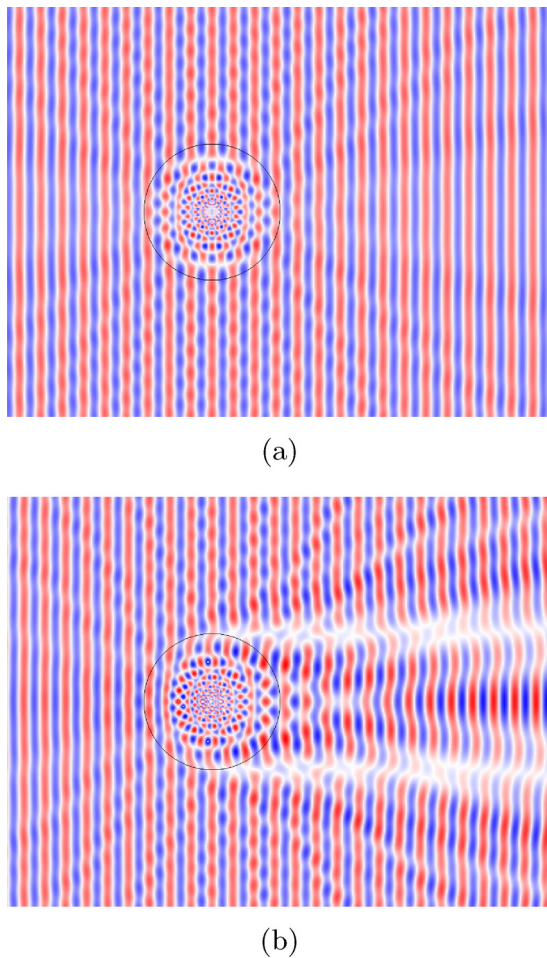


FIG. 4. (Color online) Plot of the waves resulting from illumination of the 2D invisible lens by a plane wave for (a)  $\omega = 20$  and (b)  $\omega = 20.5$ .

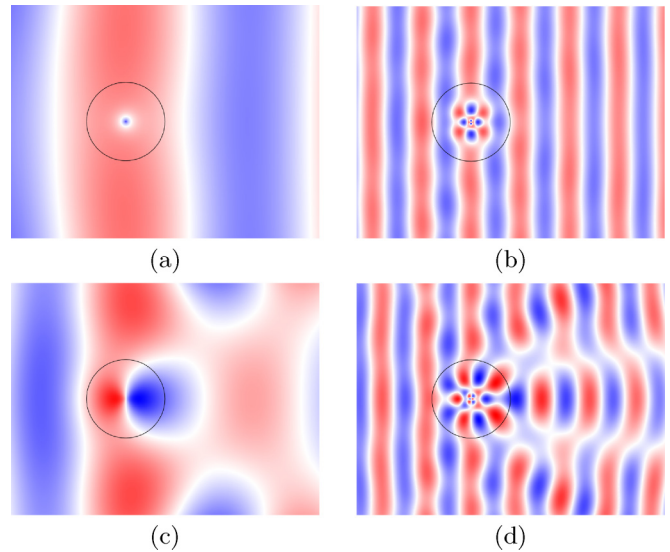


FIG. 5. (Color online) Wave simulation corresponding to exactly the same situation and parameters as Fig. 3 using the software COMSOL.

To verify our results by an independent method, we have also performed simulations of the invisible lens illuminated by plane waves by two different numerical methods. In particular, we used simulations by the finite-element method implemented by the commercial software COMSOL (see Fig. 5), and the finite-difference time-domain (FDTD) free software MEEP [15] (see Fig. 6). We see that the agreement of the three methods is quite good. In particular, our semianalytical method and COMSOL simulations give almost identical results. The MEEP simulations differ slightly, which we ascribe to numerical errors. However, the overall character of scattering by the invisible lens remains unchanged also in the MEEP simulations.

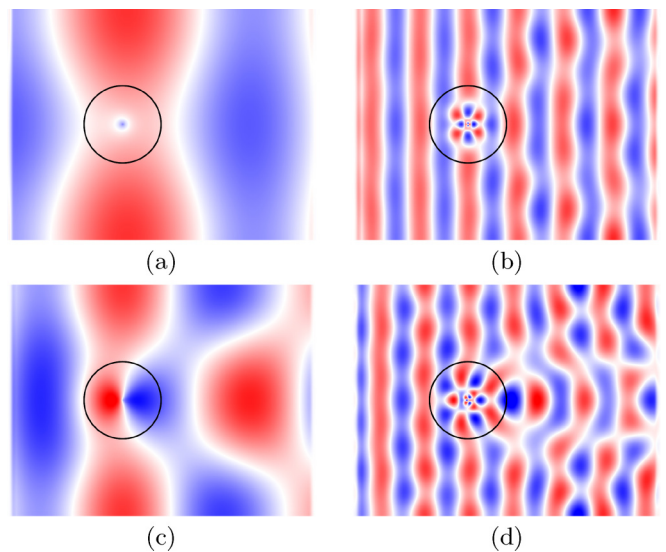


FIG. 6. (Color online) Wave simulation corresponding to exactly the same situation and parameters as Fig. 3 using the software MEEP [15].

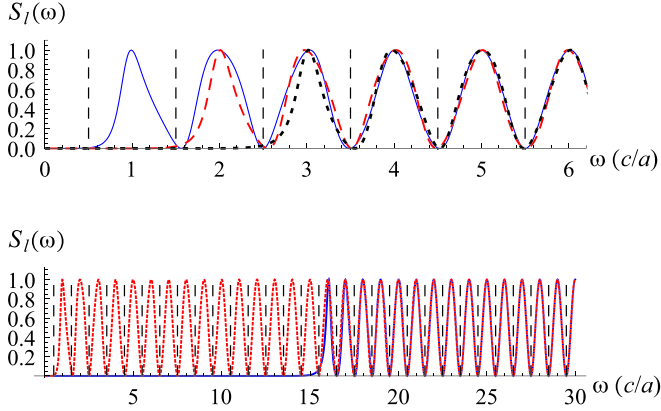


FIG. 7. (Color online) The coefficients  $S_l(\omega)$  for different values of  $l = 0, 1, 2$  (top: full blue line, dashed red line, and dotted black line, respectively) and  $m = 0, 15$  (bottom: dotted red line and full blue line, respectively) on a larger interval of frequencies. The vertical dashed lines mark the half-integer frequencies for which constructive interference occurs.

#### IV. 3D INVISIBLE LENS

Next we proceed to the 3D case. For simplicity, we will analyze the behavior of scalar waves in the 3D invisible lens; as we will see at the end of Sec. V, the general properties of scattering by an invisible lens depend very little on the type of waves.

In the 3D case, instead of Bessel and Hankel functions, we have to use spherical Bessel and Hankel functions; the angular part of the wave is now described by spherical harmonics  $Y_{lm}(\theta, \varphi)$ . Similarly to the 2D case, a plane wave can be expressed as a superposition of these spherical waves [16], in analogy to Eq. (3). When the plane wave propagates along the  $z$  axis, only the waves with  $m = 0$  will be present in the superposition. Following the completely analogous procedure, we calculate the coefficients of the scattered diverging spherical wave  $h_l^{(1)}(kr)Y_{l0}(\theta, \varphi)$  as  $S_l = \cos^2(\alpha_l/2)$ , where  $\alpha_l$  is the phase shift of the component  $h_l^{(1)}(kr)$  introduced by the presence of the invisible lens. The coefficients  $S_l(\omega)$  calculated numerically for several values of  $l$  are shown in Fig. 7. Apparently and maybe a bit surprisingly, now it is the half-integer frequencies for which  $S_l(\omega)$  are small instead of the integer ones, which was the case for  $S_m(\omega)$  (Fig. 2). This

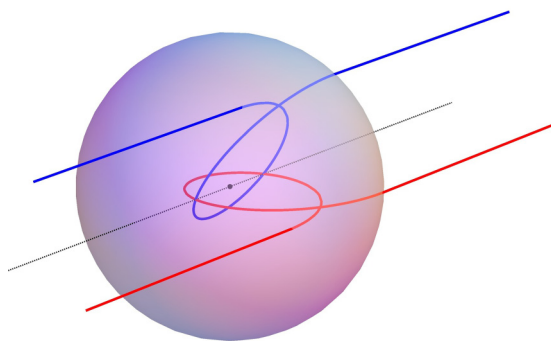


FIG. 8. (Color online) Two rays initially parallel to the  $z$  axis (black dashed line) entering the lens with the same impact parameter intersect each other twice on the  $z$  axis.

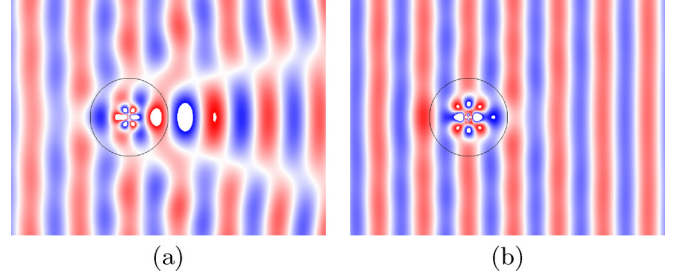


FIG. 9. (Color online) Plot of the scalar waves in the 3D invisible lens for (a)  $\omega = 5$  and (b)  $\omega = 5.5$ . Here there is a phase slip along the shadow boundary for the integer  $\omega$ , while the lens is practically invisible for half integer  $\omega$  due to the effect of the Gouy phase.

suggests the existence of some additional phase factor of  $\pi$  compared to the 2D case that the waves pick up (or lose) when they propagate through the lens. As we will show now, this factor is indeed present and is due to the Gouy phase.

#### V. GOUY PHASE

Consider two rays parallel to the  $z$  axis entering the lens with the same impact parameter; see Fig. 8. Each of these rays lies in a plane that contains the  $z$  axis. This axis is therefore also the intersection line of these two planes, and since the rays have the same impact parameter, they must intersect each other at two points on the  $z$  axis; see Fig. 8. On the other hand, two parallel rays with different impact parameters lying in a plane containing the  $z$  axis would not intersect. We see that in this way the invisible lens performs a certain type of focusing, but only in one direction, i.e., similar to the effect of a cylindrical lens: a bunch of initially parallel rays of a circular cross section would assume a linear cross section in the lens when crossing the  $z$  axis. It is well known that there is a Gouy phase factor of  $\pi/2$  connected with this type of cylindrical focusing [17]. Multiplying this factor by two because the focusing occurs twice, we find that the wave will indeed be shifted by an additional phase factor of  $\pi$ .

Figure 9 shows the plot of the scalar waves in the 3D invisible lens. As we could now expect, for integer frequencies, there is a phase slip of  $\pi$  at the boundary of the shadow, while for half integer  $\omega$ , the invisibility of the lens is almost perfect.

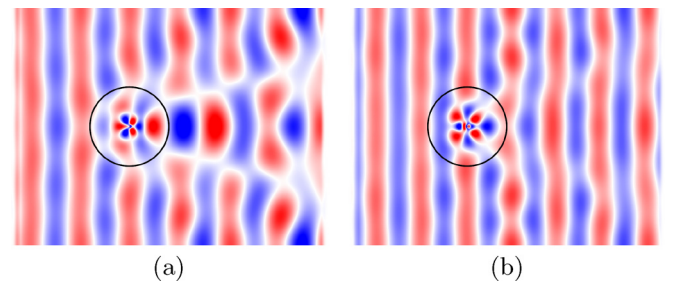


FIG. 10. (Color online) MEEP simulations for the 3D invisible lens. The frequencies correspond to Fig. 9: (a)  $\omega = 5$ , (b)  $\omega = 5.5$ . The full vector description of the waves by Maxwell's equations was employed and the electric field of the incoming plane wave was perpendicular to the plane of the image.

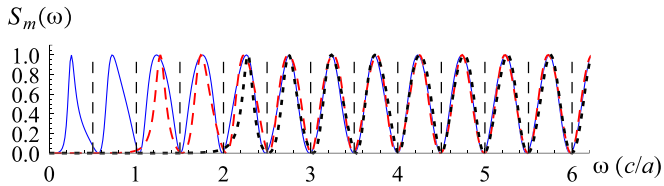


FIG. 11. (Color online) The coefficients  $S_m(\omega)$  for the double invisible lens for  $m = 0, 1, 2$  (full blue line, dashed red line, and dotted black line, respectively).

Figure 10 shows the wave simulations for the 3D invisible lens by the software MEEP. In contrast to Fig. 9, the MEEP simulations were performed for the full vector description of the waves by Maxwell's equations. The incoming wave is polarized such that the electric field is perpendicular to the plane of Fig. 10, and the refractive index is realized by purely dielectric properties of the material (i.e.,  $\mu_r = 1$ ). We see that the character of the scattering is very similar to that for scalar waves in Fig. 9, which shows that the performance of the invisible lens does not depend much on the type of waves. We did not perform simulations of this situation by COMSOL because it was challenging to handle the 3D situation with sufficient resolution.

## VI. OTHER INVISIBLE LENSES

The invisible lens discussed so far is only one representative of a whole class of lenses with a similar behavior. We can force the ray to make not just one, but an arbitrary number of loops inside the lens by choosing a suitable refractive index. An example of the “double invisible lens” with two loops is shown in Fig. 1(b). The refractive index can be calculated, e.g., by the methods explained in Refs. [9,18]. Since the delay of the ray now corresponds to twice the circumference of the lens, the constructive interference will occur when this distance is covered by an integer number of wavelengths, i.e., for  $\omega = Nc/(2a)$ ,  $N \in \mathbb{N}$ . The behavior of coefficients  $S_m(\omega)$  perfectly confirms this—they are very small for both integer

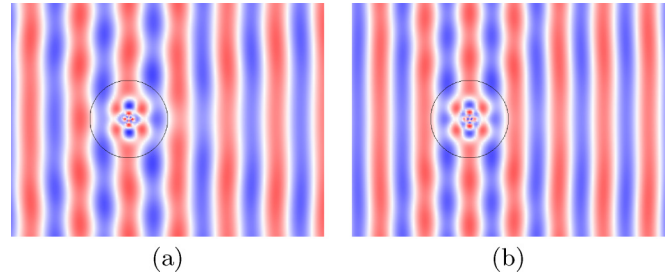


FIG. 12. (Color online) Plot of the waves in the 2D double invisible lens for (a)  $\omega = 5$  and (b)  $\omega = 5.5$ . In both cases, the interference is constructive and the lens is almost perfectly invisible.

and half-integer frequencies; see Fig. 11. Plots of the waves in the 2D double invisible lens are shown in Fig. 12.

## VII. CONCLUSION

In conclusion, we have demonstrated that the invisible lens is almost perfectly invisible for light waves for a discrete set of frequencies for which the constructive interference condition is satisfied. This condition is different in the 2D and 3D case due to the effect of the Gouy phase. The slight imperfection is unavoidable due to the theorem of the uniqueness of the inverse-scattering problem for waves [14]. The invisible lens is the only known isotropic device with a positive refractive index with invisible properties.

## ACKNOWLEDGMENTS

T.T. acknowledges support of the Grant No. P201/12/G028 of the Czech Science Foundation, and of the QUEST program grant of the Engineering and Physical Sciences Research Council. H.C. acknowledges support of the National Science Foundation of China for Excellent Young Scientists (Grant No. 61322504) and the Foundation for the Author of National Excellent Doctoral Dissertation of China (Grant No. 201217). A.D. acknowledges support from a Tier 1 grant under the Singapore Ministry of Education Academic Research Fund.

- 
- [1] U. Leonhardt, *Science* **312**, 1777 (2006).
  - [2] J. B. Pendry, D. Schurig, and D. R. Smith, *Science* **312**, 1780 (2006).
  - [3] U. Leonhardt and T. Tyc, *Science* **323**, 110 (2009).
  - [4] J. S. Li and J. B. Pendry, *Phys. Rev. Lett.* **101**, 203901 (2008).
  - [5] X. Chen, Y. Luo, J. Zhang, K. Jiang, J. B. Pendry, and S. Zhang, *Nat. Commun.* **2**, 176 (2011).
  - [6] J. Perczel, T. Tyc, and U. Leonhardt, *New J. Phys.* **13**, 083007 (2011).
  - [7] A. Alù and N. Engheta, *Phys. Rev. E* **72**, 016623 (2005).
  - [8] H. Chen, C. T. Chan, and P. Sheng, *Nat. Mater.* **9**, 387 (2010).
  - [9] A. Hendi, J. Henn, and U. Leonhardt, *Phys. Rev. Lett.* **97**, 073902 (2006).
  - [10] J. C. Miñano, *Opt. Express* **14**, 9627 (2006).
  - [11] T. Tyc and U. Leonhardt, *New J. Phys.* **10**, 115038 (2008).
  - [12] T. Tyc, H. Chen, C. T. Chan, and U. Leonhardt, *IEEE J. Sel. Top. Quantum Electron.* **16**, 418 (2010).
  - [13] H. Chen, U. Leonhardt, and T. Tyc, *Phys. Rev. A* **83**, 055801 (2011).
  - [14] A. I. Nachman, *Ann. Math.* **128**, 531 (1988).
  - [15] A. F. Oskooi, D. Roundy, M. Ibanescu, P. Bermel, J. D. Joannopoulos, and S. G. Johnson, *Comput. Phys. Commun.* **181**, 687 (2010).
  - [16] L. D. Landau and E. M. Lifshitz, *Quantum Mechanics* (Pergamon, New York, 1991).
  - [17] T. D. Visser and E. Wolf, *Opt. Commun.* **283**, 3371 (2010).
  - [18] M. Šarbot and T. Tyc, *J. Opt.* **14**, 075705 (2012).